

## Strongly Inhibited Transport of a Degenerate 1D Bose Gas in a Lattice

C. D. Fertig,<sup>1,2</sup> K. M. O'Hara,<sup>1,\*</sup> J. H. Huckans,<sup>1,2</sup> S. L. Rolston,<sup>1,2</sup> W. D. Phillips,<sup>1,2</sup> and J. V. Porto<sup>1</sup>

<sup>1</sup>National Institute of Standards and Technology, Gaithersburg, Maryland 20899-8424, USA

<sup>2</sup>University of Maryland, College Park, Maryland 20742, USA

(Received 15 November 2004; published 1 April 2005)

We report the observation of strongly damped dipole oscillations of a quantum degenerate 1D atomic Bose gas in a combined harmonic and optical lattice potential. Damping is significant for very shallow axial lattices (0.25 photon recoil energies), and increases dramatically with increasing lattice depth, such that the gas becomes nearly immobile for times an order of magnitude longer than the single-particle tunneling time. Surprisingly, we see no broadening of the atomic quasimomentum distribution after damped motion. Recent theoretical work suggests that quantum fluctuations can strongly damp dipole oscillations of a 1D atomic Bose gas, providing a possible explanation for our observations.

DOI: 10.1103/PhysRevLett.94.120403

PACS numbers: 03.75.Kk, 05.60.Gg, 73.43.Nq

The ability of highly degenerate quantum systems to sustain dissipationless flow is one of the most striking manifestations of quantum mechanics. However, transport in such systems can be dramatically modified by the presence of a relatively weak but rapidly spatially varying (“corrugated”) potential along the transport axis. For example, the periodic potential of an optical lattice inhibits transport in a degenerate Fermi atomic gas [1–3], but not, in general, in a degenerate Bose gas [i.e., Bose-Einstein condensate (BEC)] [4,5]. However, under certain conditions, highly dissipative transport in a BEC in an optical lattice [6–8] can arise from nonlinear dynamical instabilities [9–11]. In low dimensional systems, of which 1D atomic gases [12–16] and superconducting nanowires [17] are important experimentally realized examples, a corrugated potential can cause dramatic changes in ground state and transport properties.

We study inhibited transport in a 1D Bose gas in the presence of an optical lattice along the 1D axis. In the absence of such a lattice, dipole oscillations are undamped [14], since it is a general result that the dipole mode of a harmonically confined gas is unaffected by two-body interactions (generalized Kohn’s theorem) [18]. This result does not strictly hold for a combined harmonic and periodic potential; nevertheless, undamped oscillations have been observed in 3D BECs for small amplitudes and weak interactions [5,19].

In this Letter, we report a study of strongly damped dipole oscillations of a 1D Bose gas in a combined harmonic and periodic potential, under conditions for which undamped motion has been observed previously for 3D BECs. This striking difference between one dimension and three dimensions was recently reported qualitatively in Ref. [13]. Here we measure the damped motion as a function of axial lattice depth. Significant damping is induced by very shallow lattices, and in deeper lattices the motion is overdamped to the degree that the gas is nearly immobile for times an order of magnitude longer than the single-particle tunneling time. We emphasize, and discuss further below, that the inhibited transport is not due

to Bloch oscillations [4,20], where transport is frustrated by Bragg reflection at the Brillouin zone (BZ) boundary, as has been seen in previous experiments [1,2,7].

Our method to realize an ensemble of independent 1D Bose gases is similar to earlier work [12]. We produce a nearly pure <sup>87</sup>Rb condensate of  $N = (0.8\text{--}1.6) \times 10^5$  atoms in the  $|F = 1, m_F = -1\rangle$  state in a Ioffe-Pritchard magnetic trap ( $\nu_x = \nu_z = 29$  Hz,  $\nu_y = 8$  Hz). We next partition the BEC into an array of independent, vertical 1D “tubes” by adiabatically applying a transverse (in the  $xy$  plane) 2D confining lattice [12–16,21]. The confining lattice is ramped on during 200 ms to a depth of approximately  $30E_R$  (where  $E_R = h^2/2m\lambda^2$  is the photon recoil energy, and  $\lambda$  is the laser wavelength). The combined magnetic and optical potential results in approximately 5000 occupied tubes, each with an axial frequency of  $\omega_0/2\pi \approx 60$  Hz. We observe a Thomas-Fermi density envelope in the combined magnetic and optical potential, and calculate [12] cloud radii of  $r_x = 14(1) \mu\text{m}$  [22],  $r_y = 20(1) \mu\text{m}$ , and  $r_z = 10.6(5) \mu\text{m}$  for  $N = 1.4 \times 10^5$ . From this, we estimate a peak 1D density of  $4.8(4) \times 10^4 \text{ cm}^{-1}$  in the central tube, and a peak 3D density of  $4.7(4) \times 10^4 \text{ cm}^{-3}$ . Subsequently, we corrugate the tubes by adiabatically applying, over 20 ms, an axial (vertically along  $z$ ) 1D lattice. The Rayleigh length of the axial lattice beams is large enough that they do not significantly modify the axial harmonic potential. All lattice beams derive from a single Ti:Sapphire laser operating at  $\lambda = 810$  nm, far detuned from the atomic resonances at 780 and 795 nm. The pairs of lattice beams are detuned from each other by 6 MHz, making them effectively independent [23]. The final configuration consists of three independent standing waves, each formed from a pair of counterpropagating beams.

We excite dipole oscillations of the center of mass of the atoms in all the tubes by suddenly ( $\leq 150 \mu\text{s}$ ) applying a linear magnetic field gradient, thus displacing the total harmonic trap (but not the lattice) axially by  $z_0 \approx 3 \mu\text{m}$ . This displacement is less than 30% of  $r_z$  and corresponds to approximately eight axial lattice sites [24]. The waists of the Gaussian transverse lattice beams

( $w_0 \approx 210 \mu\text{m}$ ) are much larger than both  $z_0$  and the size of the trapped cloud.

The oscillation in the position of the atoms is too small for our imaging system to clearly resolve. We therefore observe oscillation in *velocity* by waiting a variable time  $t_w$  after the initial displacement, then suddenly turning off all trapping potentials (with time constants of  $\approx 250 \mu\text{s}$  and  $\approx 150 \mu\text{s}$  for the optical and magnetic potentials, respectively), and imaging the position  $z_{\text{TOF}}$  of the atoms after a time of flight (TOF)  $t_{\text{TOF}} = 18.4 \text{ ms}$ . The velocity of the atoms at  $t_w$  is found by simple kinematics, and is approximately given by  $z_{\text{TOF}}/t_{\text{TOF}}$ . The turn-off of the optical lattice is fast compared to the oscillation period, but slow enough to avoid diffraction of the atoms (i.e., adiabatic with respect to band excitations).

We observe damped dipole oscillations for axial lattice depths from  $V = 0E_R$  to  $2E_R$ , as seen in Fig. 1. In the absence of an axial lattice, we observe oscillations (period  $T = 15.4 \text{ ms}$ ) consistent with no damping [Fig. 1(a)], indicating that tube-to-tube dephasing and trap anharmonicities are not significant on the time scale of our experiments. However, the oscillations are noticeably damped in a lattice only  $0.25E_R$  deep. Such a shallow lattice modulates the atomic density by only 6%, and modifies the single-particle energy-quasimomentum dispersion relation  $E(q)$  from that of a free particle around only the last few percent of the BZ. [We note here, and discuss further below, that the amplitude of motion is kept well within the quadratic part of  $E(q)$  for shallow lattices.]

Beyond a lattice depth of  $\approx 3E_R$  the motion is overdamped, and there are no oscillations. In this case, the atoms' velocity can be quite small, so we use a technique that maps the atoms' *position* in the trap to the cloud position after TOF. The experiment proceeds as before, except that after the trap is displaced by  $z_0$ , the atoms are allowed to relax toward their equilibrium position at  $z = 0$  for a fixed time  $t_w = 90 \text{ ms}$ . We then rapidly (with time

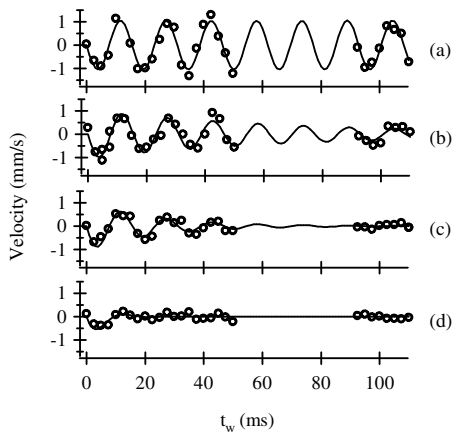


FIG. 1. Damped oscillations of a 1D Bose gas in an optical lattice. Shown are plots of velocity versus wait time  $t_w$  from  $t_w = 0$  to 110 ms, and for axial lattice depths of (a)  $0E_R$ , (b)  $0.25E_R$ , (c)  $0.50E_R$ , and (d)  $2.0E_R$ , where  $E_R$  is the photon recoil energy (see text).

constant  $\approx 250 \mu\text{s}$ ) turn off *only the axial lattice*. The remaining transverse lattice and magnetic potentials are left on for 3.75 ms (approximately a quarter period of undamped axial harmonic motion), then turned off simultaneously (as in the underdamped experiment). This converts the axial displacement  $z(t_w)$  into a velocity, which we measure by TOF.

Figure 2(a) shows  $z(t_w = 90 \text{ ms})$  as a function of axial lattice depth. For the shallowest lattices, this wait time is sufficient for the atoms to damp to the equilibrium position  $z = 0$ . For the deepest lattices, the motion is so overdamped that there is negligible motion during this time, and the position remains  $z \approx z_0$ . We note that, in the absence of damping, atoms would tunnel through the lattice to the equilibrium position in a time  $(T/4)\sqrt{m^*/m}$ , where  $m^*$  is the effective mass. This time is only 8 ms for noninteracting particles in a  $10E_R$  lattice. A comparison can also be made to the tunneling time from the Mathieu function treatment of band structure,  $4h/\Delta E = 15 \text{ ms}$ , where  $\Delta E$  is the height of the band.

To quantify the damping, we model the motion as damped simple harmonic,  $m^*\ddot{z} = -b\dot{z} - kz$ , and extract a damping constant  $b = b(V)$  for different axial lattice depths  $V$ . For underdamped motion, we simultaneously fit the oscillation data for eight depths to the expression

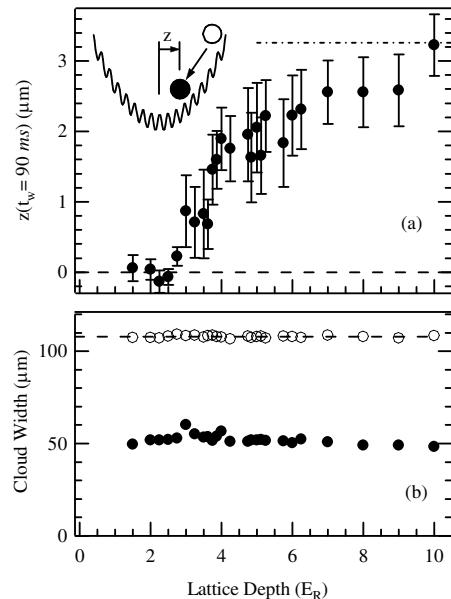


FIG. 2. Overdamped motion of a 1D Bose gas in an optical lattice. (a) Plot of the atoms' position 90 ms after shifting the trap, as a function of lattice depth. Inset depicts relaxation of the atoms toward equilibrium. Immediately after the trap is displaced to  $z_0$ , the atoms (open circle) begin to move toward equilibrium, reaching a displacement  $z$  from equilibrium after 90 ms (solid circle). Also shown is the initial position of the atoms (dash-dotted line). (b) The  $1/e$  half-widths of Gaussian fits to axial TOF distributions (solid symbols), and the half-widths of square transverse TOF distributions (open symbols) resulting from a uniformly filled BZ (see text, and Fig. 4). Also shown (dashed line) is the BZ calculated from lattice parameters.

$$\dot{z}(t) = A \frac{k}{\omega m^*} e^{-bt/2m^*} \sin(\omega t),$$

where  $\omega \equiv \sqrt{k/m^* - (b/2m^*)^2}$ , and  $A$  and  $k$  are fit parameters common across all  $V$ . For overdamped motion, we determine  $b = b(V)$  from the overdamped solution for  $z(t_w)$ , which in the limit of strong damping simplifies to

$$z(t_w) \approx z_0 \left( \frac{e^{-kt_w/b}}{1 - km^*/b^2} + \frac{e^{-bt_w/m^*}}{1 - b^2/km^*} \right),$$

where  $z_0$  and  $k$  are inputs derived from measurements of undamped oscillations. In our analysis, we use a single-particle calculation of the effective mass  $m^*$  [26].

Figure 3 shows a plot of  $b(V)/b_0$  versus lattice depth  $V$ , where  $b_0 \equiv 2m\omega_0$  corresponds to critically damped harmonic motion for  $\omega_0 \equiv \sqrt{k/m}$ . We show data for both the underdamped and overdamped regimes, and note that the damping constant increases by at least a factor 1000 for a 30-fold increase in lattice depth.

The axial width of the cloud after TOF can provide information about the distribution of atomic quasimomenta in the lattice. The lattice turn-off time constant of  $250 \mu\text{s}$  is long enough to avoid diffraction, but short enough to be nonadiabatic with respect to interwell tunneling and interactions. (Related experiments in 2D [21] and 3D [25] lattices support this conclusion.) In the absence of interactions, and neglecting the initial size of the cloud, the turn-off maps the single-particle quasimomentum distribution of atoms in the lattice to free-particle (i.e., plane-wave) momentum states that can be directly observed in TOF. In the presence of interactions, the mapping is complicated by mean-field repulsion during TOF. A variational calculation [27] indicates that mean-field repulsion is in fact the dominant contributor to the axial TOF width in our system. Therefore, the extracted TOF width greatly overestimates the width of a narrow initial quasimomentum distribution.

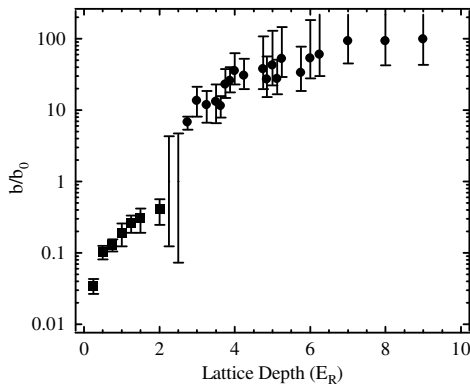


FIG. 3. Plot of the reduced damping constant  $b/b_0$  for various depths  $V$  of the axial lattice, as determined using the underdamped (squares) and overdamped (circles) experimental techniques. Near critical damping ( $V \approx 3E_R$ ), the analysis cannot distinguish between underdamped and overdamped motion, so only upper and lower bounds are shown at  $V = 2.25$  and  $2.50$ .

An example TOF image is shown in Fig. 4, together with cross-sectional profiles of the optical depth along the axial and transverse directions. The first BZ of the transverse lattice is uniformly filled, producing a uniform, square spatial distribution (in the  $xy$  plane) after TOF. Our imaging system views this square distribution along the diagonal in the  $xy$  plane, resulting in a triangular profile, from which we extract the width of the square [open symbols, Fig. 2(b)]. In the axial direction the distribution is narrower and reasonably well fit to a Gaussian, from which we extract the axial (along  $z$ ) TOF  $1/e$  half-width [solid symbols, Fig. 2(b)]. Even for the strongly overdamped data, the axial TOF width (which, we recall, overstates the width of narrow quasimomentum distributions) is much narrower than the BZ. This implies that the inhibition of transport is not due to effects related to Bloch oscillations of a filled BZ, as observed in Refs. [1,7]. Furthermore, we do not see a significant difference in TOF width between atoms that undergo damped harmonic motion and those that are unexcited but held for an equal time [28]. This is in stark contrast to earlier experiments on 3D BECs [6,8,11], where strong damping was accompanied by a pronounced broadening and fragmentation of the quasimomentum distribution.

Large amplitude dipole oscillations in a lattice can damp due to dynamical instabilities caused by particle interactions. For a 3D BEC moving in an optical lattice, such an instability point occurs at  $q \geq q_\pi/2$  ( $q_\pi \equiv 2\pi/\lambda$  is the BZ boundary), where the dispersion relation has an inflection point, as predicted in [9,10] and observed in [6,8,11]. This effect is manifested as a large increase in the width of the quasimomentum distribution. Here, in contrast, we keep the maximum (single-particle) quasimomentum  $q_{\text{max}}$  of the oscillation small by limiting the initial energy of displacement  $E(z_0) = m\omega_0^2 z_0^2/2$ . For  $V < 2E_R$ , our choice of  $z_0$  corresponds to  $q_{\text{max}} \approx q_\pi/5$ . For deeper lattices, our fixed  $z_0$  corresponds to a larger  $q_{\text{max}}$ , but is always less than  $q_\pi/2$  for  $V < 9E_R$ . (In a separate experiment, we excited oscillations in our system with twice the usual amplitude, and saw stronger damping that was ac-

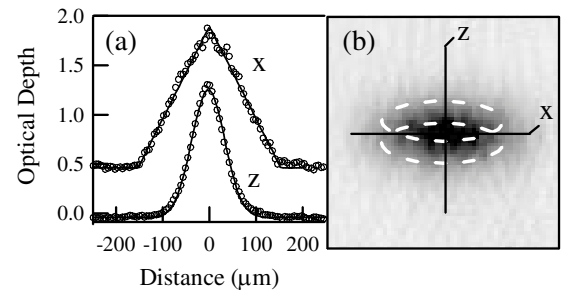


FIG. 4. Cross sections (a) of a TOF absorption image (b) of the expanded atom cloud. The plot of the transverse cross section (along  $x$ ) is offset vertically by 0.5 units for clarity. The solid lines are Gaussian (triangular) fits to the axial (transverse) profiles, respectively. The dashed ovals in (b) indicate the peak-to-peak range of motion of undamped dipole oscillations.

accompanied by a broadening of the axial TOF width by nearly a factor of 2.)

For small amplitude dipole oscillations ( $q_{\max} \ll q_{\pi}/2$ ) of a 3D BEC in an optical lattice, the effect of the lattice is merely to increase the effective mass, leading to undamped motion at a lower frequency [5,19]. In the reduced dimensionality system of our 1D Bose gas, we have seen that the optical lattice has a qualitatively different effect. To highlight the difference between these two situations, we excited dipole oscillations in a 3D BEC (i.e., *no* transverse confining lattice) in a  $4E_R$  axial lattice, and saw no damping. This is in contrast to the results of the same experiment in a 1D Bose gas (i.e., *with* a transverse confining lattice), shown in Fig. 3, where  $b(V = 4E_R)/b_0 \approx 50$  corresponds to extremely overdamped motion.

After we performed these experiments, theoretical treatments appeared which suggested that zero-temperature quantum fluctuations can lead to substantial damping of transport in a 1D atomic Bose gas [29,30]. Our observations, including the significant damping in lattices too shallow to support a Mott-insulator phase [31], can be explained by the mechanisms of Refs. [29,30], but appear to be inconsistent with a mechanism involving incompressibility [13].

It is possible that there is a temperature dependence to the damping; unfortunately, we can derive little information on temperature from the TOF widths. Future experiments to investigate the temperature dependence could shed light on the relative importance of quantum and thermal fluctuations to dissipation, a question of interest in, for example, the development of ultrathin superconducting wires [17]. We also look forward to testing other explicit predictions of these theories, such as the dependence of damping on displacement and dimensionality. We note that the periodic potential of an optical lattice is free from defects, and that 1D atomic Bose gases are well isolated from the environment, yielding a relatively clean system in which to compare experiment with theory. The ability to continuously and dynamically vary the confining potentials makes optical lattice experiments attractive for future studies of superfluidity in low dimensional quantum systems.

The authors gratefully acknowledge helpful discussions with Ana-María Rey, Julio Gea-Banacloche, and Guido Pupillo. This work was partially supported by ARDA.

---

\*Current address: Department of Physics, Pennsylvania State University, University Park, PA 16802, USA.

[1] G. Modugno *et al.*, Phys. Rev. A **68**, 011601(R) (2003).  
[2] L. Pezzè *et al.*, Phys. Rev. Lett. **93**, 120401 (2004).

- [3] H. Ott *et al.*, Phys. Rev. Lett. **92**, 160601 (2004).  
[4] O. Morsch *et al.*, Phys. Rev. Lett. **87**, 140402 (2001).  
[5] F. S. Cataliotti *et al.*, Science **293**, 843 (2001).  
[6] S. Burger *et al.*, Phys. Rev. Lett. **86**, 4447 (2001); B. Wu and Q. Niu, Phys. Rev. Lett. **89**, 088901 (2002); S. Burger *et al.*, *ibid.* **89**, 088902 (2002).  
[7] F. Ferlaino *et al.*, Phys. Rev. A **66**, 011604(R) (2002).  
[8] F. S. Cataliotti *et al.*, New J. Phys. **5**, 71 (2003).  
[9] B. Wu and Q. Niu, Phys. Rev. A **64**, 061603 (2001).  
[10] A. Smerzi, A. Trombettoni, P. G. Kevrekidis, and A. R. Bishop, Phys. Rev. Lett. **89**, 170402 (2002).  
[11] L. Fallani *et al.*, Phys. Rev. Lett. **93**, 140406 (2004).  
[12] B. L. Tolra *et al.*, Phys. Rev. Lett. **92**, 190401 (2004).  
[13] T. Stöferle *et al.*, Phys. Rev. Lett. **92**, 130403 (2004).  
[14] H. Moritz, T. Stöferle, M. Köhl, and T. Esslinger, Phys. Rev. Lett. **91**, 250402 (2003).  
[15] B. Parades *et al.*, Nature (London) **429**, 277 (2004).  
[16] T. Kinoshita, T. Wenger, and D. S. Weiss, Science **305**, 1125 (2004).  
[17] A. Bezryadin, C. N. Lau, and M. Tinkham, Nature (London) **404**, 971 (2000).  
[18] F. Dalfovo, S. Giorgini, L. Pitaevskii, and S. Stringari, Rev. Mod. Phys. **71**, 463 (1999).  
[19] M. Krämer, L. Pitaevskii, and S. Stringari, Phys. Rev. Lett. **88**, 180404 (2002).  
[20] M. BenDahan *et al.*, Phys. Rev. Lett. **76**, 4508 (1996).  
[21] M. Greiner *et al.*, Phys. Rev. Lett. **87**, 160405 (2001).  
[22] Error bars here and everywhere else represent the uncorrelated combination of 1 standard deviation statistical and systematic uncertainties (if any).  
[23] S. L. Winoto, M. T. DePue, N. E. Bramall, and D. S. Weiss, Phys. Rev. A **59**, R19 (1999).  
[24] For all lattice depths, the maximum site-to-site potential difference of 40 Hz is much less than both the on-site interaction energy and the tunneling energy, so that the transport studied in this work is fundamentally different from the excitations due to potential gradients reported in Ref. [25].  
[25] M. Greiner *et al.*, Nature (London) **415**, 39 (2002).  
[26] For overdamped motion, the extracted damping constants  $b$  depend very weakly on  $m^*/m$ . For underdamped motion, the shallowness of the axial lattice means corrections to  $m^*$  due to interactions should be small. Therefore we expect all extracted damping constants  $b$  to be insensitive to corrections to  $m^*$  due to interactions.  
[27] A. M. Rey (private communication).  
[28] During the  $\sim 100$  ms in which we observe the cloud's motion, we observe a small growth in the width of the TOF image, at a rate that is independent of excitation or damping, consistent with heating due to spontaneous scattering of lattice photons.  
[29] A. Polkovnikov and D.-W. Wang, Phys. Rev. Lett. **93**, 070401 (2004).  
[30] J. Gea-Banacloche *et al.*, cond-mat/0410677.  
[31] C. Kollath, U. Schollwöck, J. von Delft, and W. Zwerger, Phys. Rev. A **69**, 031601(R) (2004).